

Osmotic Water Permeability of Small Intestinal Brush-Border Membranes

Howard J. Worman* and Michael Field**

Departments of Medicine and of Pharmacological & Physiological Sciences, Pritzker School of Medicine, University of Chicago, Chicago, Illinois 60637

Summary. A stopped-flow nephelometric technique was used to examine osmotic water flow across small intestinal brush-border membranes. Brush-border membrane vesicles (BBMV) were prepared from rat small intestine by calcium precipitation. Scattered 500 nm light intensity at 90° to incident was a linear function of the number of vesicles in suspension, and of the reciprocal of the suspending medium osmolality. When BBMV were mixed with hyperosmotic mannitol solutions there was a rapid increase in the intensity of scattered light that could be fit to a single exponential function. The rate constant for vesicle shrinking varied with temperature and the size of the imposed osmotic gradient. At 25°C and an initial osmotic gradient of 50 mOsm, the rate constant was $1.43 \pm 0.044 \text{ sec}^{-1}$. An Arrhenius plot of the temperature dependence of vesicle shrinking showed a break at about 25°C with an activation energy of $9.75 \pm 1.04 \text{ kcal/mole}$ from 11 to 25°C and $17.2 \pm 0.55 \text{ kcal/mole}$ from 25 to 37°C. The pore-forming antibiotic gramicidin increased the rate of osmotically driven water efflux and decreased the activation energy of the process to $4.51 \pm 0.25 \text{ kcal/mole}$. Gramicidin also increased the sodium permeability of these membranes as measured by the rate of vesicle reswelling in hyperosmotic NaSCN medium. Gramicidin had no effect on mannitol permeability. Assuming spherical vesicles of 0.1 μm radius, an osmotic permeability coefficient of $1.2 \times 10^{-3} \text{ cm/sec}$ can be estimated for the native brush-border membranes at 25°C. These results are consistent with the solubility-diffusion model for water flow across small intestinal BBMV but are inconsistent with the existence there of large aqueous pores.

Key Words small intestine · brush-border membrane vesicles · water transport · stopped-flow kinetics · gramicidin

Introduction

The pathways for osmotic water flow across the small intestinal epithelium are not well defined. Relative contributions of paracellular and transcellular

pathways to total water flow remain unsettled and may be influenced by the direction of flow [15]. Whether water traverses the brush-border membrane through aqueous channels or by dissolving in the lipid phase of the membrane is also unclear.

Stopped-flow kinetic measurements of light scattering or absorbance have been used to study osmotic water flow in red blood cells [26] and in liposomes [24]. More recently this technique has been applied to membrane vesicles from epithelial cells [23, 30, 33]. The activation energy of water flow across apical membranes from gastric parietal cells [23], for example, is much higher than that for red blood cell membranes [31], which are thought to have aqueous pores [17], and is closer to that for liposomes [24]. In the present study we have used stopped-flow nephelometry to examine osmotic water flow across rat small intestinal brush borders in the presence and absence of gramicidin A.

Materials and Methods

VESICLE PREPARATION

Male Lewis rats, obtained from Charles River Breeding Laboratory (Boston, Mass.), were anesthetized with ether and then killed by cardiac puncture. The distal 4/5 of the small intestine was removed and rinsed with ice-cold 0.9% NaCl. The mucosa was separated from the underlying musculature by scraping with a glass slide. The mucosa was then homogenized in a Waring blender for 90 sec and brush-border membrane vesicles were isolated by a Ca^{2+} precipitation method previously described [11]. The final brush-border pellet was suspended in 100 mM mannitol, 1.0 mM Tris-HEPES buffer (pH 7.4) and stored unfrozen at 0 to 4°C for no longer than 30 hr prior to use. Protein content was determined by the Lowry method [16] after solubilization of the membranes in 1.0 N NaOH. Alkaline phosphatase activity was measured spectrophotometrically by the hydrolysis of *p*-nitrophenolphosphate at pH 8.5 in the presence of MgCl_2 [12]. The specific activity of the alkaline phosphatase was 13- to 15-fold enriched in the brush-border pellet when compared to the

* Present address: Department of Medicine, Cornell University Medical College, New York, N.Y. 10021.

** Present address: Division of Gastroenterology, Department of Medicine, Columbia University College of Physicians & Surgeons, New York, N.Y. 10032.

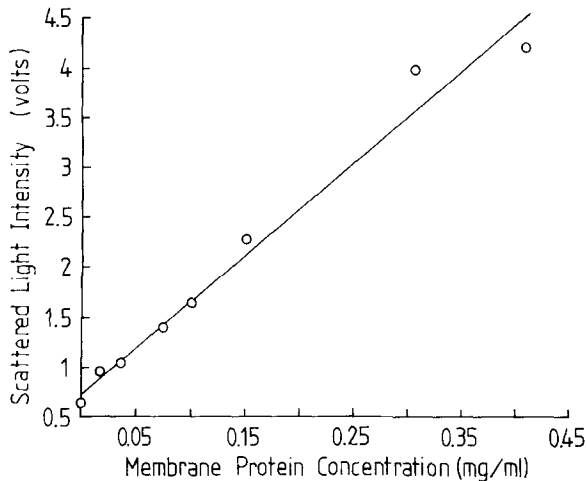


Fig. 1. Plot of 500 nm scattered light intensity at 90° to incident versus protein concentration of brush-border membrane vesicle suspensions. Values on the ordinate are photomultiplier output voltages. Identical suspensions of vesicles were placed in both drive syringes of the stopped-flow apparatus, the vesicle concentrations being varied to yield the desired protein concentrations. The suspending buffer was 100 mM mannitol, 1.0 mM Tris-HEPES (pH 7.4), and the temperature was 25°C

original homogenate. Four brush-border preparations yielded a mean specific activity of 1.34 ± 0.21 (1 SEM) units protein mg.

STOPPED-FLOW NEPHELOMETRIC MEASUREMENTS

These were made at 90° to incident using 500-nm filters (Omega Optical Co., Battleboro, Vt.) with a homemade stopped-flow apparatus, the construction of which has been previously described [9]. One drive syringe of the stopped-flow device was loaded with a suspension of brush-border vesicles (0.15 to 1.0 mg protein per ml) in 100 mM mannitol, 1.0 mM Tris-HEPES (pH 7.4). The other drive syringe was loaded with the desired hyper- to iso-osmotic mannitol solution buffered by 1.0 mM Tris-HEPES (pH 7.4). The two drive syringes were mixed in a one-to-one ratio by a plunger driven by compressed air. The intensity of 90° scattered light was measured by a photomultiplier tube and displayed on a digital voltmeter and an oscilloscope. The intensity of scattered light versus time was stored in digital form on a Digital PDP 11/10 computer (Digital Equipment Corporation, Maynard, Mass.) and plotted using a Hewlett-Packard 7015A X-Y recorder (Hewlett-Packard Company, Palo Alto, Calif.) Exponential rate constants were calculated using a nonlinear least-squares program. A desired constant temperature was maintained with a circulating water bath and monitored with a thermocouple probe placed in close proximity to the reaction cuvette.

TREATMENT OF BRUSH-BORDER VESICLES WITH GRAMICIDIN

Gramicidin was dissolved in methanol to a concentration of 3 mg/ml and added to brush-border suspensions. The final methanol concentration was always less than 0.1%. The gramicidin-

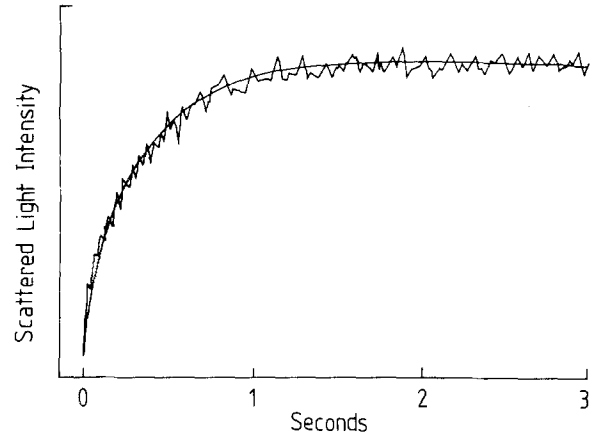


Fig. 2. Scattered light intensity (arbitrary units) as a function of time for a suspension of brush-border membrane vesicles maintained at 30°C and exposed at time zero to a 175 mM hyperosmotic gradient. Also shown is the best-fitting single exponential function determined by the method of least squares. Scattered light intensity was measured at 90° to incident at wavelength of 500 nm. One drive syringe of the stopped-flow apparatus contained vesicles (concentration = 0.2 mg protein per ml) suspended in 100 mM mannitol, 1.0 mM Tris-HEPES (pH 7.4); the other drive syringe contained 450 mM mannitol and 1.0 mM Tris-HEPES. The contents of the two drive syringes were mixed in a 1:1 ratio yielding a protein concentration of 0.1 mg/ml, an initial intravesicular solution containing 100 mM mannitol and an initial extravesicular solution containing 275 mM mannitol

containing suspensions were heated to 42°C for several minutes to insure incorporation of gramicidin into the membranes.

MATERIALS

Mannitol, CaCl_2 , and methanol were obtained from Fisher (Fair Lawn, N.J.). HEPES, Tris base, *p*-nitrophenolphosphate, NaSCN, and gramicidin from *Bacillus brevis* were obtained from Sigma (St. Louis, Mo.). Commercial gramicidin (about 85% gramicidin A) from *Bacillus brevis* was used without further purification.

Results

USE OF LIGHT SCATTERING TO MEASURE OSMOTIC WATER FLOW IN VESICLE SUSPENSIONS

The intensity of scattered light, measured at a wavelength of 500 nm and recorded at 90° to incident, proved linearly proportional to the concentration of membrane protein to at least $400 \mu\text{g/ml}$ (Fig. 1). When a vesicle suspension was mixed with a mannitol solution of higher osmolality the intensity of light scattering increased, taking several seconds to reach a new steady state (Fig. 2). Scattered light intensity then remained constant for at least one

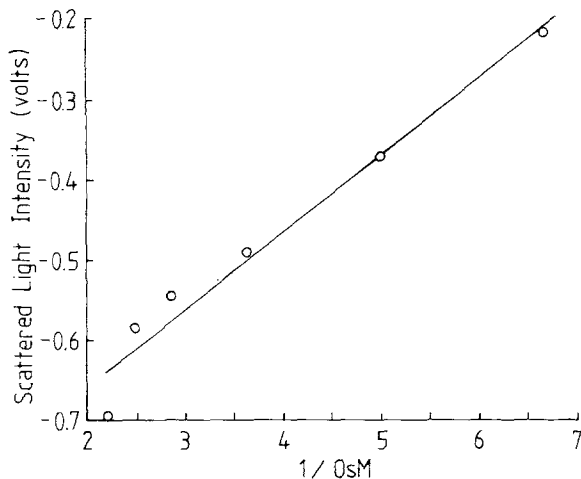


Fig. 3. Intensity of 500-nm scattered light versus reciprocal of medium osmolality for suspensions of brush-border membrane vesicles maintained at 25°C. The values on the ordinate are the negative of the increase in photomultiplier output voltage above that seen when vesicle suspensions were in 100 mM mannitol, 1.0 mM Tris-HEPES (pH 7.4). To obtain the desired osmolalities, one drive syringe of the stopped-flow apparatus contained 1.0 mg membrane protein per ml of 100 mM mannitol and 1.0 mM Tris-HEPES (pH 7.4) and the other drive syringe contained mannitol at a high osmolality and 1.0 mM Tris-HEPES. These were mixed in a 1:1 ratio. The photomultiplier output voltage was recorded several seconds after the new equilibrium was reached

minute, indicating that mannitol does not readily enter the vesicles since mannitol entry would cause reswelling and an attendant decrease in light scattering. The increase in scattered light intensity could be fit well by a single exponential function. Scattered light intensity was not altered when the vesicle suspension was mixed with iso-osmotic rather than hyperosmotic mannitol. When vesicles were mixed with 1.0 mM Tris-HEPES in the absence of mannitol, vesicles swelled rather than shrank and scattered light intensity decreased.

Changes in scattered light intensity proved to be linearly proportional to the reciprocal of suspending medium osmolality from 100 to 400 mOsm/liter (Fig. 3). At higher osmolalities the curve deviated from linearity. Over the linear range of osmolalities, scattered light intensity, as measured by the negative of photomultiplier voltage, can be substituted for volume in the Boyle-Van't Hoff equation,

$$V = K(1/C) + V_0 \quad (1)$$

where V is vesicle volume, V_0 is the volume below which the vesicles cannot shrink and C is the osmolality. Between 100 and 400 mOsm/liter, therefore, these vesicles behave as spherical osmometers and

Table 1. Exponential rate constant as a function of mannitol gradient^a

| Osmotic gradient (mM mannitol) | Rate constant (sec ⁻¹) |
|--------------------------------|------------------------------------|
| 50 | 1.43 ± 0.044 |
| 150 | 1.71 ± 0.150 |
| 175 | 1.74 ± 0.061 |
| 250 | 2.31 ± 0.320 |
| 350 | 3.00 ± 0.062 |

^a Rate constants were determined at 25°C by a nonlinear least-squares program on a PDP 11/10 computer. Values are means ± 1 SE for three vesicle preparations, each derived from intestines of three rats and each tested at least three times. Initial mannitol concentration was 100 mM.

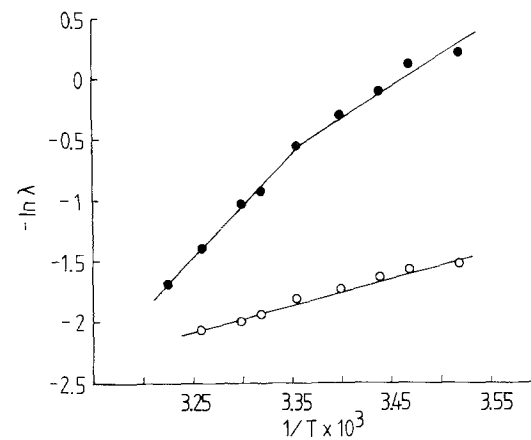


Fig. 4. Arrhenius plot of the exponential rate constants for osmotic water efflux from brush-border membrane vesicles (BBMV) with (O-O-O) and without (●-●-●) pretreatment with gramicidin (10 μg per mg membrane protein). Conditions were the same as those indicated in the legend to Fig. 2. The data for the gramicidin experiments are from two batches of BBMV, each tested at least three times at each temperature. Standard errors at each temperature are not shown but were less than 6% of the mean

changes in the intensity of scattered light can be used to measure changes in vesicle volume.

The rate constant for vesicle shrinkage and the amplitude of volume change were functions of the initial osmotic gradient. Data for rate constants are shown in Table 1. Rate constants for a particular osmotic gradient varied little from one vesicle preparation to another.

The rate constant for vesicle shrinkage was also a function of temperature as shown by the Arrhenius plots in Fig. 4. There is an apparent break in the slope at about 25°C with linearity at higher and lower temperatures. Values for the activation energies of osmotic water flow above and below 25°C are given in Table 2.

Table 2. Activation energies of osmotic water efflux in small intestinal brush-border membrane vesicles^a

| Additions | Temperature range (°C) | Activation energy (Kcal/mol) |
|-----------------------|------------------------|------------------------------|
| — | 11–25 | 9.75 ± 1.04 |
| — | 25–37 | 17.2 ± 0.55 |
| Gramicidin (10 µg/mg) | 11–37 | 4.51 ± 0.25 |
| Gramicidin (4 µg/mg) | 11–25 | 7.70 |
| Gramicidin (4 µg/mg) | 25–37 | 13.00 |

^a Values are means ± 1 SD for the slopes of the least-squares regression lines shown in Fig. 4. Values from three vesicle preparations, each derived from intestines of three rats, were obtained for control conditions and from two preparations for gramicidin at 10 µg/mg membrane protein. One vesicle preparation was tested for gramicidin at 4 µg/mg. Each vesicle preparation was tested at least three times at each temperature. A 175-mm mannitol gradient (275 mM outside and 100 mM inside) was employed.

EFFECT OF GRAMICIDIN ON OSMOTIC WATER FLOW

When the brush-border vesicles were treated with gramicidin (10 µg/mg protein), the rate of vesicle shrinkage due to osmotic water efflux increased. The effects of gramicidin on the rate constants for water efflux and on the activation energy are shown in Fig. 4. In addition to increasing the rate of water efflux at each temperature, gramicidin also decreased the activation energy of the process to 4.51 ± 0.25 kcal/mole (Table 2). The apparent break in the plot at 25°C seen with native brush-border membranes disappeared with gramicidin treatment. One batch of vesicles was treated with a lower dose of gramicidin (4 µg/mg protein). The break in the Arrhenius plot was still apparent at this concentration of gramicidin with activation energies slightly lower than those of native membranes (Table 2). Treatment of the vesicles with methanol at 1% by volume, a concentration of 10 times greater than that used to dissolve the gramicidin, had no effect on the rate of water efflux.

EFFECTS OF GRAMICIDIN ON Na⁺ AND MANNITOL PERMEABILITIES

When vesicles equilibrated with 100 mM mannitol were exposed to a solution containing 100 mM mannitol and 150 mM NaSCN, they initially shrank as indicated by the rapid increases in scattered light intensity shown in the first two tracings in Fig. 5. Thereafter, scattered light intensity gradually decreased to its baseline value. This secondary and much slower change in scattered light intensity

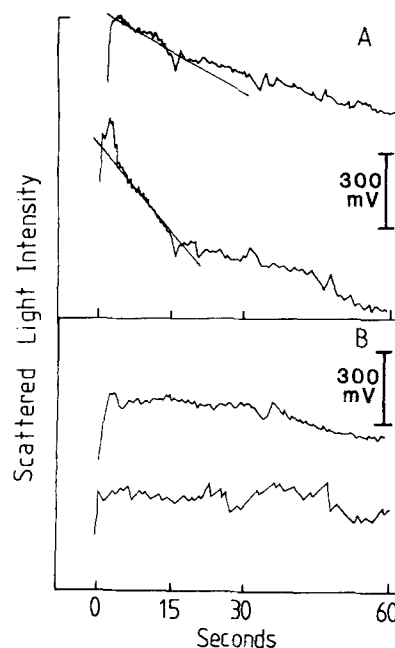


Fig. 5. Changes in scattered light intensity (photomultiplier output voltage) with time for control (upper recordings in sections A and B) and gramicidin-treated (lower recordings in each section) brush-border membrane vesicles mixed with hyperosmotic solutions of NaSCN and mannitol. In section A, syringe 1 of the stopped-flow apparatus contained 0.45 mg/ml membrane protein in 100 mM mannitol and 1.0 mM Tris-HEPES (pH 7.4), and syringe 2 contained 300 mM NaSCN, 100 mM mannitol and 1.0 mM Tris-HEPES (pH 7.4). The contents of the syringes were mixed in a 1:1 ratio yielding an initial intravesicular solution of 100 mM mannitol, 1.0 mM Tris-HEPES, and an extravesicular solution of 150 mM NaSCN, 100 mM mannitol, and 1.0 mM Tris-HEPES. The gramicidin-containing vesicles had been preincubated with 10 µg gramicidin per mg membrane protein. Temperature was maintained at 25°C. In section B, syringe 1 contained 0.43 mg/ml membrane protein in 100 mM mannitol and 1.0 mM Tris-HEPES (pH 7.4), and syringe 2 contained 540 mM mannitol and 1.0 mM Tris-HEPES (pH 7.4) and temperature was maintained at 30°C.

measures vesicle reswelling as NaSCN enters the intravesicular space and water follows osmotically. When pretreated with gramicidin (10 µg/mg protein), the vesicles reswelled more rapidly than under control conditions (compare first and second tracings in Fig. 5). This can be attributed to the gramicidin-induced increase in Na⁺ permeability since SCN⁻, a lipid-soluble anion, readily traverses the membrane and is not rate-limiting for solute entry. The bottom two tracings in Fig. 5 show changes in light scattering after the vesicles were exposed to 275 mM mannitol. Little reswelling took place indicating little permeability to mannitol. Furthermore, reswelling was not detectably faster in gramicidin-treated membranes, indicating that gramicidin did not produce a nonspecific increase in membrane permeability to all small aqueous solutes.

Table 3. Activation energies of osmotic water flow in cells and in artificial and biological membranes vesicles

| System | Activation energy (kcal/mole) | Reference |
|--|-------------------------------|-------------------------------|
| Human polymorphonuclear leukocytes | 18.4 | Hempling, 1973 [8] |
| Small intestinal brush border (25–37°C) | 17.2 | Present study |
| Human chronic leukemic lymphocytes | 16.3 | Hempling, 1973 [8] |
| Mouse ova, unfertilized | 14.5 | Leibo, 1980 [13] |
| Gastric plasma membrane vesicles | 13.9 | Rabon et al., 1980 [23] |
| Calf lymphocytes | 13.1 | Hempling, 1973 [8] |
| Mouse ova, fertilized | 13.0 | Leibo, 1980 [13] |
| Sea urchin ova | 13–17 | McCutcheon & Lucke, 1932 [19] |
| Chicken red blood cells | 11.4 | Farmer & Macey, 1970 [5] |
| Small intestine brush border (11–25°C) | 9.75 | Present study |
| Lecithin liposomes | 8.6 | Cohen, 1975 [3] |
| Lecithin liposomes | 8.25 | Reeves & Dowben, 1970 [24] |
| Small intestinal brush border + gramicidin (11–34°C) | 4.5 | Present study |
| Bovine red blood cells | 4.0 | Farmer & Macey, 1970 [5] |
| Canine red blood cells | 3.7 | Vieira et al., 1970 [31] |
| Human red blood cells | 3.3 | Vieira et al., 1970 [31] |

Discussion

Although the increases in light scattering with time after exposure of brush-border vesicles to an osmotic gradient could be fit to a single exponential, the curve in Fig. 2 most likely represents a mean function for a group of vesicles that are somewhat heterogeneous with respect to size and permeability. Nonetheless, with the help of a few assumptions, we can estimate the average osmotic permeability of rat small intestine brush-border membrane vesicles. Farmer and Macey [5] have shown that for small osmotic gradients, the hydraulic conductivity L_p is related to the exponential time constant for cell swelling or shrinking by the equation

$$\tau = \frac{(1-b)V_o}{RTC_o L_p A} \pi^{-2} \quad (2)$$

where τ is the exponential time constant for cell shrinkage, V_o the initial cell volume, C_o the initial osmolality, A the cell surface area, π the ratio of final to initial osmolality, and b the fraction of cell volume that is not water. For initially spherical vesicles that maintain a relatively constant surface area during osmotic shrinkage, and neglecting $(1-b)$, Eq. (2) reduces to

$$RTL_p = \frac{\lambda r_o \pi^{-2}}{3C_o} \quad (3)$$

where λ is the exponential rate constant ($1/\tau$) and r_o is the initial radius. Kedem and Katchalsky [10] have defined the hydraulic conductivity L_p , which they related to the commonly used permeability coefficient P_f by the equation

$$P_f = \frac{RTL_p}{\bar{V}_m} \quad (4)$$

where \bar{V}_m is the molar volume of liquid water (18 cm³/mole). If we use the value of λ for the smallest osmotic gradient in Table 1, and if we assume spherical brush-border vesicles with an average radius of 0.1 μ m in 100 mM mannitol [11], the estimated value of P_f for small intestinal brush-border vesicles is 1.2×10^{-3} cm/sec at 25°C. This value may represent somewhat of an overestimate since we have neglected $(1-b)$, which may be significant due to the presence of brush-border core material, and have assumed spherical vesicles, which have the smallest surface-to-volume ratio. The value is less than that of 4.4×10^{-3} cm/sec obtained for lecithin liposomes at 25°C [24] and less than 10% of that obtained for mammalian red blood cells at 25°C [5, 26].

The mechanism and pathway for osmotic water flow across the brush-border membrane is suggested by the activation energies of osmotic water flow found in the literature for various biological and artificial membrane systems (Table 3). Activation energies in the range of 4 kcal/mole were only seen with mammalian red blood cells. Values between 4 and 5 kcal/mole have been determined for the activation energy of the viscosity of water and for the diffusion of ³H₂O in bulk water [32], and are consistent with transmembrane water flow through large aqueous pores [3, 7, 17, 22, 31]. In mammalian red blood cells, considerable evidence exists, other than the low activation energy, for aqueous pores as the predominant pathway for water transport [17]. In synthetic lipid bilayer membranes, which do not

contain large aqueous pores, values for the activation energy of osmotic water flow between 11 and 14 kcal/mole have been reported [22]. These higher values are also seen in most biological membrane systems as well as synthetic liposome vesicles and are consistent with the so-called solubility-diffusion model for water translocation across membranes [3, 22, 24]. In the solubility-diffusion model, the activation energy for transmembrane water flow is determined by the energies required for water molecules to break hydrogen bonds with their neighbors in the aqueous phase on one side of the membrane, dissolve in the membrane, diffuse across it, and form hydrogen bonds again on the opposite side of the membrane. The values for the activation energies of osmotic water flow across small intestinal brush-border membranes are consistent with the solubility-diffusion model for transmembrane water flow and suggest the absence of large aqueous pores.

The effects of gramicidin A also support the hypothesis that transmembrane water flow through large aqueous pores yields an activation energy for the process around 4 kcal/mole similar to that for the viscosity and diffusion of bulk water [17, 31, 32]. Gramicidin A forms transmembrane pores that are able to act as channels for some cations [29] and for water [25], and has been shown to increase the osmotic water permeability of synthetic liposomes [3] and black lipid membrane [25]. It also has been shown to decrease the activation energy for osmotic water flow in phospholipid liposomes from its usually high value down to about 4 kcal/mole [1]. In these liposome preparations the apparent break in the Arrhenius plots of water flow, that is normally seen at the lipid phase transition temperature, also disappeared when gramicidin was incorporated [1]. The value of 4.51 kcal/mole seen after treatment of intestinal brush-border vesicles with gramicidin (10 $\mu\text{g}/\text{mg}$ membrane protein) suggests that, under these conditions, almost all of the transmembrane water flow occurs via large aqueous channels created by gramicidin A. Gramicidin (4 $\mu\text{g}/\text{mg}$ membrane protein) reduced the activation energy seen in the native membranes from 17.2 to 13 kcal/mole at temperatures above 25°C, suggesting that intermediate activation energies for water flow can be seen when both solubility-diffusion through the proteolipid bilayer and flow through aqueous channels are quantitatively significant. Gramicidin incorporation (10 $\mu\text{g}/\text{mg}$ membrane protein) also abolished the break in the slope of the Arrhenius plot for water flow that was seen at 25°C in native brush-border membrane vesicles. The beginning of a broad low-enthalpy lipid phase transition has previously been reported to occur at about 25°C in rat small intestinal brush-border membranes [2], and the occur-

rence of a break in the Arrhenius plot of osmotic water flow in brush-border vesicles at the same temperature suggests that when water crosses a membrane by the solubility-diffusion mechanism, the dynamics of the membrane lipids affects the water permeability properties. In the presence of large aqueous transmembrane gramicidin channels, however, the state of the membrane lipids does not appear to influence brush-border membrane water permeability as suggested by disappearance of the break in the Arrhenius plot of water flow.

The experiments in vesicle reswelling (Fig. 5) indicate that gramicidin forms channels for Na^+ and water in the membrane but does not introduce permeability to other normally excluded solutes, such as mannitol. Thus gramicidin does not appear to have a nonspecific detergent-like effect on the membrane.

Frömter and Diamond [6] originally proposed that in intact leaky epithelia such as the small intestine and gallbladder, transepithelial water flow occurs primarily via a paracellular route through the tight junctions, and that in tight epithelia, water flow occurs primarily via a transcellular route. This hypothesis has subsequently been questioned by Diamond [4] and also has been challenged by van Os, Wiedner and Wright [20] and by Spring and co-workers [21, 28], who claim that in the gallbladder, solute-linked water flow occurs primarily by a transcellular pathway. Although it is tempting to use the present measurements of brush-border vesicle water permeability to predict what the pathways are for transepithelial water flow in the intact small intestine, such extrapolations are hazardous. First of all, we are uncertain as to what effects the isolation procedure, particularly the calcium precipitation step, may have on the permeability of the native membranes. Second, our measurements on brush-border membrane vesicles do not reflect the apical membranes of cells in the intestinal crypts, which could differ in permeability appreciably [18]. Third, old literature values [14, 27] for the osmotic permeability of the intact intestine are not corrected for an unstirred layer subsequently shown to affect measurements of water permeability in leaky epithelia (*see* Diamond [4]). Finally, surface amplification factors (villus surface, for example) have not been considered. From the present experiments, we can conclude that the value of P_f for small intestinal brush-border membranes prepared by the calcium precipitation method is close to 1.2×10^{-3} cm/sec at 25°C, and that water crosses these membranes by the solubility-diffusion mechanism. The extent to which these properties of the isolated brush-border membranes contribute to overall water flow across the intact small intestine remains to be determined.

We are indebted to Dr. Edwin W. Taylor for the use of his stopped-flow apparatus and for his patience in explaining to us its design and operation. We also thank Dr. Mrinalini C. Rao for her help and advice, and Jiyong Ahn and Nancy Nash for technical assistance. This work was supported by NIH grant #AM-21345. Howard J. Worman is a recipient of the Calvin Fentress Research Fellowship Award of the Pritzker School of Medicine of the University of Chicago.

References

- Boehler, B.A., DeGier, J., Van Deenen, L.L.M. 1978. The effect of gramicidin A on the temperature dependence of water permeation through liposomal membranes prepared from phosphatidylcholines with different chain lengths. *Biochim. Biophys. Acta* **512**:480-488
- Brasitus, T.A., Tall, A.R., Schachter, D. 1980. Thermotropic transitions in rat intestinal plasma membranes studied by differential scanning calorimetry and fluorescence polarization. *Biochemistry* **19**:1256-1261
- Cohen, B.E. 1975. The permeability of liposomes to non-electrolytes. I. Activation energies for permeation. *J. Membrane Biol.* **20**:205-234
- Diamond, J.M. 1979. Osmotic water flow in leaky epithelia. *J. Membrane Biol.* **51**:195-216
- Farmer, R.E.L., Macey, R.I. 1970. Perturbation of red cell volume: Rectification of osmotic flow. *Biochim. Biophys. Acta* **196**:53-65
- Frömter, E., Diamond, J.M. 1972. Route of passive ion permeation in epithelia. *Nature New Biol.* **235**:9-13
- Gary-Bobo, C.M., Solomon, A.K. 1971. Effect of geometrical and chemical constraints on water flux across artificial membranes. *J. Gen. Physiol.* **57**:610-622
- Hempling, H.G. 1973. Heats of activation for the exosmotic flow of water across the membrane of leukocytes and leukemic cells. *J. Cell. Physiol.* **81**:1-10
- Johnson, K.A., Taylor, E.W. 1978. Intermediate states of subfragment I and actosubfragment I ATPase: Reevaluation of the mechanism. *Biochemistry* **17**:3432-3442
- Kedem, O., Katchalsky, A. 1958. Thermodynamic analysis of the permeability of biological membranes to non-electrolytes. *Biochim. Biophys. Acta* **27**:229-246
- Kessler, M., Acuto, O., Storelli, C., Murer, H., Muller, M., Semenza, G. 1978. A modified procedure for the rapid preparation of efficiently transporting vesicles from small intestinal brush border membranes. Their use in investigating some properties of D-glucose and choline transport systems. *Biochim. Biophys. Acta* **506**:136-154
- Langridge-Smith, J.E., Field, M., Dubinsky, W.P. 1983. Isolation of transporting plasma membrane vesicles from bovine tracheal epithelium. *Biochim. Biophys. Acta* **731**:318-328
- Leibo, S.P. 1980. Water permeability and its activation energy of fertilized and unfertilized mouse ova. *J. Membrane Biol.* **53**:179-188
- Lindemann, B., Solomon, A.K. 1962. Permeability of luminal surface of intestinal mucosal cells. *J. Gen. Physiol.* **45**:801-810
- Loeschke, K., Bentzel, C.J., Csaky, T.Z. 1970. Asymmetry of osmotic flow in frog intestine: Functional and structural correlation. *Am. J. Physiol.* **218**:1723-1731
- Lowry, O.H., Rosebrough, N.J., Farr, A.L., Randall, R.J. 1951. Protein measurement with the Folin phenol reagent. *J. Biol. Chem.* **193**:265-275
- Macey, R.I. 1984. Transport of water and urea in red blood cells. *Am. J. Physiol.* **246**:C195-C203
- Marcial, M.A., Carlson, S.L., Madara, J.L. 1984. Partitioning of paracellular conductance along the ileal crypt-villus axis: A hypothesis based on structural analysis with detailed consideration of tight junction structure-function relationships. *J. Membrane Biol.* **80**:59-70
- McCutcheon, M., Lucke, B. 1932. The effect of temperature on permeability to water of resting and activated cells (unfertilized and fertilized) eggs of *Arbacia punctulata*. *J. Cell. Comp. Physiol.* **2**:11-26
- Os, C.H. van, Wiedner, G., Wright, E.M. 1979. Volume flows across gallbladder epithelium induced by small hydrostatic and osmotic gradients. *J. Membrane Biol.* **49**:1-20
- Persson, B., Spring, K.R. 1982. Gallbladder epithelial cell hydraulic water permeability and volume regulation. *J. Gen. Physiol.* **79**:481-505
- Price, H.D., Thompson, T.E. 1969. Properties of lipid bilayer membranes separating two aqueous phases: Temperature dependence of water permeability. *J. Mol. Biol.* **41**:443-457
- Rabon, E., Takeguchi, N., Sachs, G. 1980. Water and salt permeability of gastric vesicles. *J. Membrane Biol.* **53**:109-117
- Reeves, J.P., Dowben, R.M. 1970. Water permeability of phospholipid vesicles. *J. Membrane Biol.* **3**:123-141
- Rosenberg, P.A., Finkelstein, A. 1978. Water permeability of gramicidin A-treated lipid bilayer membranes. *J. Gen. Physiol.* **72**:341-350
- Sha'afi, R.I., Rich, G.T., Sidel, V.W., Bossert, W., Solomon, A.K. 1967. The effect of the unstirred layer on human red cell water permeability. *J. Gen. Physiol.* **50**:1377-1399
- Smyth, D.H., Wright, E.M. 1966. Streaming potentials in the rat small intestine. *J. Physiol. (London)* **182**:591-602.
- Spring, K.R., Ericson, A.-C. 1982. Epithelial cell volume modulation and regulation. *J. Membrane Biol.* **69**:167-176
- Urry, D.W. 1972. A molecular theory of ion-conducting channels: A field-dependent transition between conducting and nonconducting conformations. *Proc. Natl. Acad. Sci. USA* **69**:1610-1614
- Verkman, A.S., Dix, J.A., Seifter, J.L. 1984. Water and urea permeability in brush border membrane vesicles (BBMV) measured by light scattering. *Kidney Int.* **25**:320
- Vieira, F.L., Sha'afi, R.I., Solomon, A.K. 1970. The state of water in human and dog red cell membranes. *J. Gen. Physiol.* **55**:451-466
- Wang, J.H., Robinson, C.V., Edelman, I.S. 1953. Self-diffusion and structure of liquid water. III. Measurement of the self-diffusion of liquid water with H², H³ and O¹⁸ as tracers. *J. Am. Chem. Soc.* **75**:466-470
- Worman, H.J., Field, M. 1984. Osmotic water flow in brush border vesicles from rat small intestine. *Fed. Proc. Fed. Am. Soc. Exp. Biol.* **43**:315

Received 22 March 1985; revised 18 June 1985